JOURNAL OF AGRICULTURAL AND FOOD CHEMISTRY

pubs.acs.org/JAFC Article

Synthesis, Biological Evaluation, and 3D-QSAR Studies of *N*-(Substituted pyridine-4-yl)-1-(substituted phenyl)-5-trifluoromethyl-1*H*-pyrazole-4-carboxamide Derivatives as Potential Succinate Dehydrogenase Inhibitors

Zhibing Wu,[‖] Hyung-Yeon Park,[‖] Dewen Xie, Jingxin Yang, Shuaitao Hou, Nasir Shahzad, Chan Kyung Kim,* and Song Yang*

Cite This: *J. Agric. Food Chem.* 2021, 69, 1214−1223 Read Online

ACCESS | Metrics & More | Article Recommendations | Supporting Information

ABSTRACT: A series of new fungicides that can inhibit the succinate dehydrogenase (SDH) was classified and named as SDH inhibitors by the Fungicide Resistance Action Committee in 2009. To develop more potential SDH inhibitors, we designed and synthesized a novel series of *N*-(substituted pyridine-4-yl)-1-(substituted phenyl)-5-trifluoromethyl-1*H*-pyrazole-4-carboxamide derivatives, **4a**−**4i**, namely, **5a**−**5h**, **6a**−**6h**, and **7a**−**7j**. The bioassay results demonstrated that some title compounds exhibited excellent antifungal activity against four tested phytopathogenic fungi (*Gibberella zea*, *Fusarium oxysporum*, *Cytospora mandshurica*, and *Phytophthora infestans*). The EC_{50} values were 1.8 μg/mL for **7a** against *G. zeae*, 1.5 and 3.6 μg/mL for **7c** against *F. oxysporum* and *C. mandshurica*, respectively, and 6.8 μg/mL for **7f** against *P. infestans*. The SDH enzymatic activity testing revealed that the IC_{50} values of **4c**, **5f**, **7f**, and penthiopyrad were 12.5, 135.3, 6.9, and 223.9 μg/mL, respectively. The molecular docking results of this series of title compounds with SDH model demonstrated that the compounds could completely locate inside of the pocket, the body fragment formed H bonds, and the phenyl ring showed a π−π interaction with Arg59, suggesting that these novel 5-trifluoromethyl-pyrazole-4-carboxamide derivatives might target SDH. These results could provide a benchmark for understanding the antifungal activity against the phytopathogenic fungus *P. infestans* and prompt us to discover more potent SDH inhibitors.

KEYWORDS: *5-trifluoromethyl-1H-pyrazole-4-carboxamide derivatives, fungicidal activity, succinate dehydrogenase, 3D-QSAR, ligand docking*

INTRODUCTION

A series of novel fungicides that can inhibit succinate dehydrogenase (SDH) was classified and named as SDH inhibitors (SDHIs) by the Fungicide Resistance Action Committee in 2009.[1] From 1969 to 2020, 22 SDHI fungicides have been commercialized (Figure 1). Among these compounds, carboxin, a narrow-spectrum fungicide, was first marketed in 1969 and has special activity against basidiomycetes but limited activity toward other plant pathogenic fungi.[2−8] Amide bonds are the core feature of SDHIs, and considering the introduction of structurally diverse benzene rings and heterocycles on both sides of the amide bond, compounds exhibit good broad spectrum activity; boscalid, which was introduced in 2003, was the first compound with a truly broad spectrum activity.[9,10] SDHI fungicides have been growing rapidly since 2009, and 13 commercialized products have been released,[11−14] including 10 products with a pyrazole carboxamide structure. The structural analysis of these 10 SDHIs demonstrated that all the pyrazole rings only have a CH_3 substituent at the 1-position, six of them have CHF_2 or CF_3 substituents at the 3-position, and four have two different substituents at the 3- and 5-positions of the pyrazole ring. However, none of them have substituents solely at the 5-position of the pyrazole ring.

The target of SDHIs is the SDH complex in the respiratory chain.[1] SDH is composed of four distinct subunits, including two hydrophilic subunits SDH A and SDH B (iron−sulfur subunits) in the peripheral domain and two hydrophobic membrane-spanning subunits, SDH C (Cytochrome b_L) and SDH D (Cytochrome b_S).[15,16] Mechanism research has indicated that all the SDHIs could inhibit fungal respiration by binding to the ubiquinone-binding site (UQ-site) of the mitochondrial SDH complex II in the electron transport chain, and this site is a functional part of the tricarboxylic acid cycle.[3,4,17,18] The UQ-site is formed by residues from subunits SDH B, C, and D near the [3Fe−4S] cluster and heme b and is highly conserved in bacteria and eukaryotes.[5,19−22]

On the basis of the active skeleton of 5-trifluoromethyl-4-pyrazole carboxamide, which was first found by us,[23,24] a series of novel *N*-(substituted-pyridine-4-yl)-1-(substituted phenyl)-5-trifluoromethyl-1*H*-pyrazole-4-carboxamide derivatives was

Received: September 4, 2020
Revised: December 11, 2020
Accepted: January 15, 2021
Published: January 22, 2021

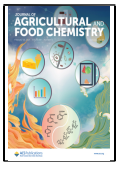

Downloaded via UNIV OF PRINCE EDWARD ISLAND on May 15, 2021 at 13:54:54 (UTC).
See https://pubs.acs.org/sharingguidelines for options on how to legitimately share published articles.

ACS Publications © 2021 American Chemical Society

https://dx.doi.org/10.1021/acs.jafc.0c05702
J. Agric. Food Chem. 2021, 69, 1214−1223

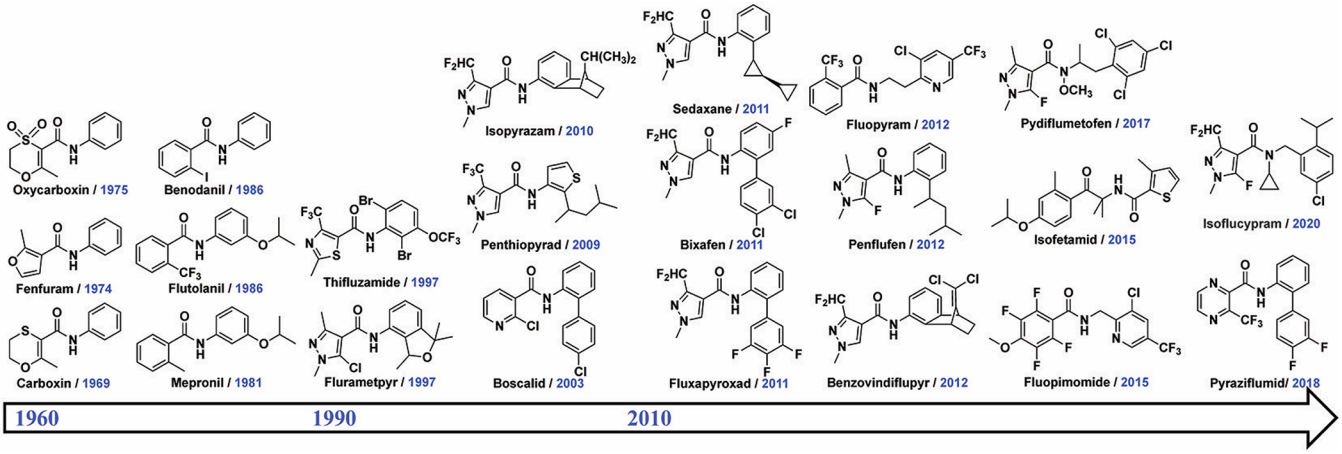

Figure 1. Commercialised SDHI fungicides from 1969 to 2020.

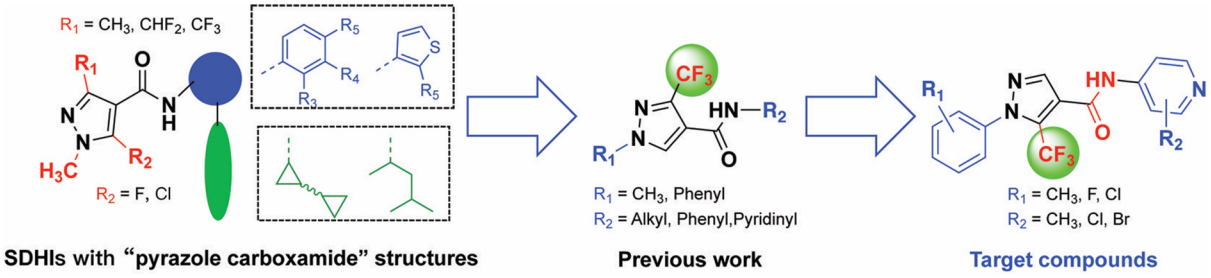

Figure 2. Design of title compounds.

designed and synthesized (Figures 2 and 3). The *in vitro* antifungal activity results revealed that some title compounds

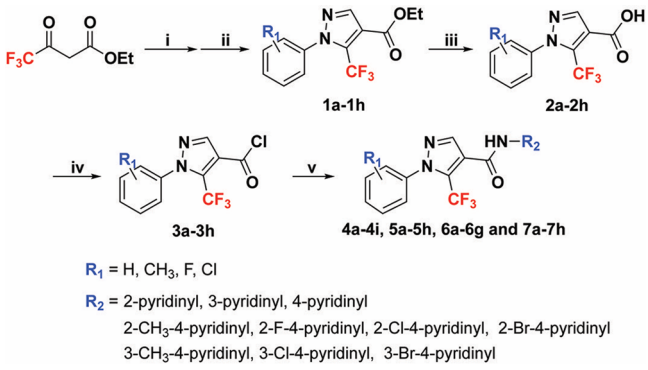

Figure 3. Synthetic route of the title compounds **4a−4i**, **5a−5h**, **6a−6h**, and **7a−7j**. Reagents and conditions: (i) $CH(OEt)_3$, Ac_2O; (ii) substituted phenylhydrazine, EtOH; (iii) LiOH, THF/H_2O; (iv) $SOCl_2$; and (v) substituted pyridine amine, NaH, anhydrous THF.

exhibited excellent antifungal activity against four kinds of pathogenic fungi. SDH enzymatic bioassay indicated that the title compounds have better enzyme inhibition effects than commercial products penthiopyrad and carboxin. Furthermore, molecular docking results revealed the binding modes of the 5-trifluoromethyl-1*H*-pyrazole-4-carboxamide derivatives, thus providing key information for the design of SDHI fungicides.

MATERIALS AND METHODS

Instruments and Chemicals. ^{1}H NMR, ^{13}C NMR, and ^{19}F NMR spectra were taken on a JEOL-500 (JEOL CO., Ltd., Japan) or a Bruker 400 NMR spectrometer (Bruker Corporation, Germany) with tetramethylsilane (TMS) as the internal standard and $CDCl_3$ or DMSO-d_6 as the solvents. High-resolution mass spectra (HRMS) data were obtained on a Thermo Scientific Q Exactive (Thermo Scientific, USA). Mass spectra studies were conducted by LC/MS (LC, 1100; MS, MSD Trap VL, Agilent Technologies, USA). The single crystal structure of the title compound was tested on a diffractometer (SMART-1000, Bruker Corporation, Germany). The SDH enzymatic activity data were recorded with a microplate reader (Cytation 5, BioTek Instruments, USA). Melting points were measured with XT-4 binocular microscope melting point apparatus (uncorrected). Commercialised SDHIs carboxin and penthiopyrad were bought from J&K Scientific Ltd. (Beijing, China). All reagents and solvents were of analytical grade.

Fungi. Six plant pathogenic fungi (*Gibberella zea*, *Fusarium oxysporum*, *Cytospora mandshurica*, *Thanatephorus cucumeris*, *Phytophthora infestans*, and *Botrytis cinérea*) were used for antifungal testing. All fungi were kindly provided by the College of Agriculture, Nanjing Agricultural University, Nanjing, China. These fungi were grown on potato dextrose agar (PDA) plates at 25 ± 1 °C and maintained at 4 °C.

Synthesis.[23−27] *General Procedure for the Synthesis of **1a−1h**.* A mixture of ethyl trifluoroacetoacetate (0.1 mol), triethyl orthoformate (0.2 mol), and acetic anhydride (0.3 mol) was stirred at 130 °C for 4 h. The reaction mixture was concentrated *in vacuo*. The residue was dissolved in ethanol (100 mL), and phenylhydrazine (0.1 mol) was added slowly to the solution, reacting at 100 °C for 5 h. The solvent was then removed under reduced pressure. The residue was dissolved in ethyl acetate, and the organic layer was washed with brine, dried over anhydrous Na_2SO_4, and concentrated *in vacuo*. The crude product was purified by column chromatography (PE/EA = 20/1−50/1) to obtained **1a** as a yellow oil, yield 72%. ^{1}H NMR (500 MHz, DMSO-d_6): δ 8.31 (s, 1H, pyrazole H), 7.63−7.54 (m, 5H, benzene H), 4.32 (q, J = 7.2 Hz, 2H, CH_2), 1.31 (t, J = 7.2 Hz, 3H, CH_3). MS (ESI): m/z 285 $[M + H]^+$. The physical and spectral data of **1b−1h** are provided in the Supporting Information.

https://dx.doi.org/10.1021/acs.jafc.0c05702
J. Agric. Food Chem. 2021, 69, 1214−1223

General Procedure for the Synthesis of ***2a−2h.*** To a solution of **1a** (0.03 mol) in THF (30 mL) was added lithium hydroxide (0.12 mmol), and the mixture was reacted at 80 °C for 1 h. The solution was concentrated *in vacuo*. Hydrochloric acid (2 M) was used to adjust the pH value to approximately 4, and some solid precipitated and was then filtrated. The filtrate was washed with water and dried to obtained **2a** as a yellow solid, yield 92%, mp 191−192 °C. ^{1}H NMR (500 MHz, DMSO-d_6): δ 13.38 (s, 1H, COOH), 8.25 (s, 1H, pyrazole H), 7.62−7.53 (m, 5H, benzene H). MS (ESI) m/z: 279 $[M + Na]^+$. The physical and spectral data of **2b−2h** are provided in the Supporting Information.

General Procedure for the Synthesis of ***3a−3h.*** Intermediates **3a−3h** were prepared with a previously reported procedure using $SOCl_2$ as a solvent. The solvent was removed under a vacuum after the reaction was finished, and the crude product was directly used for the next reaction.

General Procedure for the Synthesis of ***4a−4i, 5a−5h, 6a−6h, and 7a−7j.*** 4-Aminopyridine (1.0 mmol), **3a** (1.1 mmol), NaH (2.0 mmol), and anhydrous THF (5 mL) were added into a 25 mL three-neck round-bottom flask and stirred at room temperature for 4 h. The THF was removed under reduced pressure. The residue was dissolved in ethyl acetate (25 mL). Then, the organic layer was washed by brine, dried over anhydrous Na_2SO_4, and filtered. The solvent was removed under a vacuum. The residue was further purified by column chromatography on a silica gel to obtain **4c** as a white solid, yield 65%, mp 108−109 °C. ^{1}H NMR (400 MHz, $CDCl_3$): δ 8.47 (d, J = 8.0 Hz, 2H, pyridine H), 8.01 (s, 1H, pyrazole H), 7.63 (d, J = 8.0 Hz, 2H, pyridine H), 7.51−7.49 (m, 3H, benzene H and NH), 7.39 (d, J = 8.0 Hz, 2H, benzene H). ^{13}C NMR (101 MHz, $CDCl_3$): δ 160.18, 160.16, 150.51, 150.49, 145.54, 150.49, 145.54, 145.50, 139.59, 138.91, 130.33, 129.48, 125.91, 120.71, 120.49, 120.48, 118.02, 114.27, 14.36. ^{19}F NMR (376 MHz, $CDCl_3$): δ −55.56. HRMS: calcd for $C_{16}H_{11}F_3N_4O$, $[M - H]^-$ 331.08012, found 331.08090. The physical and spectral data of **4a−4i**, **5a−5h**, **6a−6h**, and **7a−7j** are provided in the Supporting Information.

Crystal Structure Determination. A single crystal of title compound **4c** was grown from EtOH. A sample of size 0.20 × 0.18 × 0.10 mm^3 was selected for the crystallographic study. The diffraction measurement was performed at a temperature of 113 K using graphite monochromated Mo Kα radiation (λ = 0.71073 Å) and an Enraf-Nonius CAD-4 four-circle diffractometer. The accurate cell parameters and orientation matrix were obtained by the least-squares refinement of the setting angles of 1472 reflections at the h range of $2.12 < \theta < 27.87$. The systematic absences and intensity symmetries indicated the orthorhombic *Pbcn* space group. Corrections for LP factors were applied. The structure was solved by direct methods and refined by full-matrix least-squares techniques on F^2 with anisotropic thermal parameters for all nonhydrogen atoms. The calculations were performed with the SHELXL-97 program.

Bioassays. The fungicidal activities of **4a−4i**, **5a−5h**, **6a−6h**, and **7a−7j** were tested *in vitro* against six plant pathogenic fungi (*G. zeae*, *F. oxysporum*, *C. mandshurica*, *T. cucumeris*, *P. infestans*, and *B. cinerea*) using a mycelial growth inhibition method.[24] The preliminary activity screening concentration of the title compounds was 100 μg/mL. The mycelia dishes of fungi that were used to for testing were cut from the PDA medium, cultivated at 25 ± 1 °C and approximately 4 mm in diameter, were inoculated in the middle of a PDA plate with a germ-free inoculation needle, and then were incubated for 4−5 days at the same temperature. DMSO (1%) in sterile distilled water served as a blank control, whereas commercialized SDHI fungicides carboxin and penthiopyrad served as the positive controls. Each treatment condition consisted of three replicates. When the mycelia of the blank control grew to 6 cm, the diameter of the mycelia treated with the title compounds was recorded. Inhibitory effects on these fungi were calculated by the formula I (%) = $[(C - T)/(C - 0.4)] \times 100$, where C represents the diameter of fungal growth of the blank control, T represents the diameter of the fungi with treated compound, and I represents the inhibition rate. Standard deviation (SD) values were calculated on the basis of the inhibition data of three repetitions for each test compound.

On the basis of the *in vitro* antifungal activity results, the median effective concentrations (EC_{50} values) of the highly active compounds were further determined according to the method described above. A series of activity screening concentrations of the title compounds and positive controls consisting of 200, 100, 50, 25, 12.5, 6.25, or 3.125 μg/mL was prepared. EC_{50} values were calculated with SPSS software 20.[27,28] The regression equations of the title compounds are provided in Tables S2 and S3 in the Supporting Information.

SDH Enzyme Assay. The SDH enzyme activities of **4c**, **5f**, **7f**, and penthiopyrad were determined by using a succinate dehydrogenase assay kit (Solarbio, BC0955) and assessed as reported previously.[29] *P. infestans* was grown in potato dextrose (PD) medium for 4 days and then treated with **4c**, **5f**, **7f**, or penthiopyrad at different concentrations (200, 100, 50, 25, 12.5, 6.25, or 3.125 μg/mL). The SDH enzymatic activity was measured after 48 h of treatment with the selected compounds, and the absorbance value was measured at 600 nm by using a microplate reader. The inhibitions values were calculated by GraphPad Prism 6.0. The EC_{50} values of the title compounds were further determined according to the method described in the Bioassays section. Differences between the groups were compared by one-way analysis of variance (ANOVA; Duncan's multiple range test) with $P < 0.05$. Statistical tests were performed using the SPSS software package (version 20).

Homology Modeling. The target protein SDH consists of four subunits (SDH A, SDH B, SDH C, and SDH D), and the UQ-site is formed by the residues from the B, C, and D subunits of SDH.[17−22] Therefore, the B, C, and D subunits of *P. infestans* SDH (*Pi*SDH) were built on the basis of the available sequence data from the NCBI database: strain B-XP_002901751.1, strain C-XP_002900462.1, and strain D-XP_002896752.1. To identify a suitable parent standard for docking, the FUGUE sequence-structure homology recognition program was used to identify protein candidate hits.[30] Alignments for the highest-scoring hits produced by FUGUE were formatted with JOY (Mizuguchi) and analyzed visually to highlight the conservation of the structurally important residues.[30,31] Profile−profile matching between the target sequence and the HOMTRAD database generated initial hits for homology recognition and alignment.[31] The model was constructed with ORCHESTRA on the basis of the result of FUGUE.[32] The model structure was validated by Protable, and visual inspection was performed using 3D graphics software.[33] The initial model was energy-minimized by the conjugate gradient method until the energy gradient norm converged to 0.01 kcal/mol.

Molecular Docking. The constructed homology model of *Pi*SDH was used for the docking study. The binding site was identified by SITEID.[34] Twenty title compounds were selected as the docking ligands, and the structures were drawn using the sketch module of the SYBYL package and minimized using the Tripos force field with the Gasteiger-Hückel charge until the RMS gradient was less than 0.05. The molecular docking studies were performed on the inhibitor−SDH interactions using SYBYL packages to examine the binding energies of the synthesized SDH inhibitor candidates.[35−37] Docking of the inhibitors was carried out using the Run-Multiple ligand option of Surflex-Dock.[3] The docking score, which estimates the free energy of binding (ΔG) for the protein−ligand complex, was calculated using a modified Böhm scoring function, which includes entropic, hydrogen bonding, ionic, aromatic, and lipophilic terms.

RESULTS AND DISCUSSION

Chemistry. The synthetic route is shown in Figure 3. Ethyl 4,4,4-trifluoro-3-oxobutanoate and triethyl orthoformate were used as the starting materials to synthesis a transition intermediate that reacted with substituted-phenyl hydrazines to obtain the key intermediates **1a−1h**. Compounds **2a−2h** were obtained from **1a−1h** through hydrolysis in the presence of lithium hydroxide and then refluxed in $SOCl_2$ to obtain **3a−3h**, which were reacted with different pyridine amines to obtain the title compounds **4a−4i**, **5a−5h**, **6a−6h**, and **7a−7j**. The key synthetic intermediates were characterized by ^{1}H

https://dx.doi.org/10.1021/acs.jafc.0c05702
J. Agric. Food Chem. 2021, 69, 1214−1223

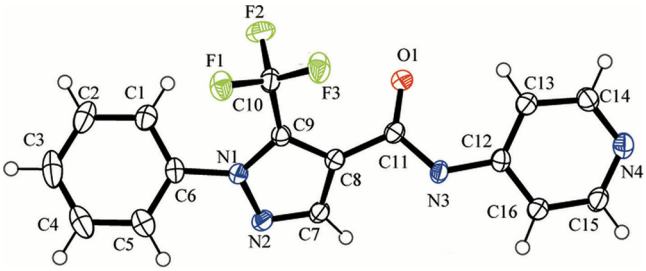

Figure 4. Single crystal structure of **4c**.

nuclear magnetic resonance (NMR) and ESI-MS, and the title compounds were characterized by ^{1}H NMR, ^{13}C NMR, ^{19}F NMR, and HRMS.

X-ray Diffraction. To confirm the trifluoromethyl functional group at the 5-position of the pyrazole ring, we determined the crystal structure of title compound **4c**. The skeleton of the new compound **4c** contains a pyrazole ring, a pyridine ring, and an amide bond connected to C(8) and C(12). The benzene ring and trifluoromethyl group are directly attached to the N(1) and C(9), respectively, which are part of the pyrazole ring (Figure 4). The C(9)—N(1) bond length (1.362 Å) was slightly longer than that of a typical C═N bond (1.34 Å), indicating a significant double bond

Table 1. Structures and Inhibition Rates of Title Compounds 4a−4i, 5a−5h, 6a−6h, and 7a−7j at 100 μg/mL on Pathogenic Fungi[a]

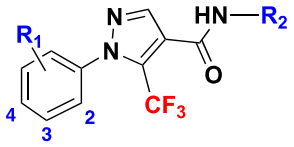

			inhibition rate (%)					
compound number	R_1	R_2	*G. zeae*	*F. oxysporum*	*C. mandshurica*	*T. cucumeris*	*P. infestans*	*B. cinerea*
4a	H	2-pyridinyl	66.9 ± 2.7	34.4 ± 1.7	28.7 ± 1.7	50.8 ± 1.1	22.8 ± 1.0	–
4b	H	3-pyridinyl	38.1 ± 2.1	20.5 ± 3.9	28.9 ± 1.0	31.4 ± 1.4	24.0 ± 0.9	57.1 ± 1.5
4c	H	4-pyridinyl	84.1 ± 1.7	93.2 ± 2.8	94.3 ± 3.5	24.1 ± 1.9	100	28.9 ± 1.1
4d	H	3-CH_3-4-pyridinyl	64.9 ± 2.9	77.5 ± 2.4	76.8 ± 2.6	19.2 ± 1.9	57.9 ± 1.7	24.3 ± 1.5
4e	H	3-Cl-4-pyridinyl	65.6 ± 1.8	77.8 ± 2.9	79.4 ± 3.2	61.6 ± 2.4	70.9 ± 1.8	–
4f	H	3-Br-4-pyridinyl	69.6 ± 1.5	75.9 ± 3.2	76.4 ± 2.5	56.9 ± 1.3	68.5 ± 2.4	–
4g	H	2-CH_3-4-pyridinyl	85.1 ± 2.3	100	100	57.8 ± 2.0	100	41.6 ± 1.1
4h	H	2-Cl-4-pyridinyl	54.6 ± 1.5	63.8 ± 1.4	69.5 ± 2.1	25.9 ± 1.3	59.1 ± 1.3	–
4i	H	2-Br-4-pyridinyl	34.5 ± 2.7	47.7 ± 1.2	63.1 ± 3.4	24.1 ± 1.1	30.8 ± 2.9	–
5a	4-Cl	4-pyridinyl	37.3 ± 1.8	26.6 ± 2.2	22.2 ± 1.4	92.9 ± 3.2	66.1 ± 3.7	77.5 ± 2.6
5b	4-Cl	3-Cl-4-pyridinyl	79.0 ± 2.1	72.9 ± 2.5	81.4 ± 2.2	72.4 ± 3.3	54.2 ± 3.1	75.4 ± 4.0
5c	4-Cl	2-CH_3-4-pyridinyl	34.6 ± 2.3	25.1 ± 1.9	35.2 ± 2.1	29.2 ± 1.8	27.8 ± 1.8	59.8 ± 3.0
5d	4-Cl	2-Cl-4-pyridinyl	19.3 ± 1.1	16.3 ± 1.1	13.5 ± 1.2	–	–	–
5e	4-CH_3	3-Cl-4-pyridinyl	44.1 ± 2.2	34.3 ± 2.2	25.9 ± 1.6	35.6 ± 2.2	35.9 ± 1.8	45.3 ± 2.9
5f	4-CH_3	4-pyridinyl	36.4 ± 2.5	27.8 ± 3.5	26.3 ± 2.1	42.0 ± 2.0	34.5 ± 3.3	72.5 ± 3.5
5g	4-CH_3	2-CH_3-4-pyridinyl	9.7 ± 1.4	9.4 ± 1.7	15.7 ± 1.5	9.6 ± 1.5	9.2 ± 1.5	72.8 ± 3.9
5h	4-CH_3	2-Cl-4-pyridinyl	5.2 ± 2.0	0	–	7.4 ± 2.9	7.0 ± 2.9	59.8 ± 3.5
6a	3-Cl	4-pyridinyl	60.2 ± 1.8	50.8 ± 1.6	54.5 ± 1.4	56.7 ± 2.3	51.6 ± 2.2	69.9 ± 4.4
6b	3-Cl	3-CH_3-4-pyridinyl	62.9 ± 2.4	37.2 ± 1.8	25.5 ± 2.2	61.5 ± 2.9	41.5 ± 2.2	68.8 ± 2.4
6c	3-Cl	3-Cl-4-pyridinyl	56.0 ± 2.0	56.2 ± 1.9	59.4 ± 2.3	77.2 ± 3.8	65.0 ± 2.6	61.2 ± 3.5
6d	3-Cl	2-CH_3-4-pyridinyl	26.9 ± 2.6	78.2 ± 3.1	66.9 ± 3.5	49.0 ± 2.4	67.6 ± 2.9	70.3 ± 3.5
6e	3-Cl	2-Cl-4-pyridinyl	15.0 ± 1.8	0	–	22.8 ± 3.9	15.5 ± 3.9	54.8 ± 2.8
6f	3-CH_3	4-pyridinyl	62.0 ± 2.6	61.0 ± 3.0	64.2 ± 2.5	49.7 ± 2.3	44.9 ± 2.4.	73.9 ± 3.4
6g	3-CH_3	2-CH_3-4-pyridinyl	62.9 ± 2.7	87.7 ± 2.8	71.0 ± 2.9	52.6 ± 2.2	46.1 ± 3.2	76.1 ± 2.6
6h	3-CH_3	2-Cl-4-pyridinyl	57.3 ± 4.2	0		10.4 ± 3.9	0	66.6 ± 3.5
7a	2-Cl	4-pyridinyl	98.4 ± 3.2	100	100	51.6 ± 2.2	100	45.7 ± 2.2
7b	2-Cl	3-Cl-4-pyridinyl	66.8 ± 2.2	87.7 ± 2.6	76.0 ± 2.7	72.1 ± 3.5	76.5 ± 3.7	59.8 ± 2.7
7c	2-Cl	2-CH_3-4-pyridinyl	88.7 ± 2.7	88.9 ± 3.3	81.7 ± 2.2	30.4 ± 1.8	77.1 ± 1.9	74.3 ± 2.8
7d	2-Cl	2-Cl-4-pyridinyl	33.7 ± 2.3	28.0 ± 1.6	–	31.7 ± 3.9	32.7 ± 4.4	61.8 ± 3.7
7e	2-F	4-pyridinyl	81.2 ± 3.7	94.6 ± 2.4	90.7 ± 3.1	31.7 ± 2.5	92.3 ± 2.5	–
7f	2-F	2-CH_3-4-pyridinyl	88.6 ± 2.7	91.0 ± 2.7	90.1 ± 3.4	90.8 ± 2.9	95.4 ± 3.2	75.6 ± 2.7
7g	2-CH_3	4-pyridinyl	90.6 ± 3.6	94.1 ± 2.3	100	36.5 ± 1.9	94.4 ± 3.8	45.7 ± 2.4
7h	2-CH_3	3-Cl-4-pyridinyl	73.2 ± 2.7	91.8 ± 3.2	86.5 ± 2.1	73.4 ± 2.4	71.2 ± 3.2	79.7 ± 1.4
7i	2-CH_3	2-CH_3-4-pyridinyl	85.3 ± 3.1	95.4 ± 3.3	80.8 ± 3.4	29.2 ± 1.8	84.3 ± 1.4	63.4 ± 2.3
7j	2-CH_3	2-Cl-4-pyridinyl	50.9 ± 2.2	66.7 ± 4.0	–	51.5 ± 3.5	74.8 ± 2.9	74.4 ± 3.0
carboxin			67.1 ± 2.7	28.4 ± 1.6	–	88.3 ± 4.3	38.1 ± 1.7	100
penthiopyrad			56.7 ± 2.3	60.0 ± 3.7	76.0 ± 3.6	100	21.2 ± 1.9	100

[a]Values are mean ± SD of three replicates. "–" not tested.

https://dx.doi.org/10.1021/acs.jafc.0c05702
J. Agric. Food Chem. 2021, 69, 1214−1223

Table 2. EC_{50} Values of Some Title Compounds against Four Kinds of Pathogenic Fungi[a]

	EC_{50}(μg/mL)			
compound number	*G. zeae*	*F. oxysporum*	*C. mandshurica*	*P. infestans*
4c	19.1 ± 1.5	24.3 ± 2.4	33.7 ± 4.1	7.9 ± 1.1
4d	57.9 ± 2.1	87.7 ± 2.7	85.8 ± 3.2	94.6 ± 2.6
4e	82.6 ± 1.5	39.8 ± 2.2	30.2 ± 1.1	70.1 ± 1.8
4f	83.5 ± 2.3	43.8 ± 2.9	44.0 ± 1.2	82.6 ± 1.7
4g	9.6 ± 1.8	8.4 ± 1.3	15.9 ± 3.5	7.2 ± 1.1
5b	39.4 ± 2.3	62.6 ± 1.4	42.6 ± 2.7	90.7 ± 3.5
5f	138.0 ± 2.7	>200	>200	>200
5g	>200	>200	>200	>200
6b	69.1 ± 3.5	>200	>200	126.5 ± 2.7
6d	>200	46.8 ± 1.6	51.1 ± 2.5	77.2 ± 2.2
6f	65.1 ± 1.9	68.1 ± 2.3	85.7 ± 2.5	132.6 ± 3.4
6g	79.0 ± 2.0	23.0 ± 1.4	48.5 ± 2.7	121.7 ± 3.5
7a	1.8 ± 0.2	9.5 ± 2.6	8.7 ± 1.4	8.9 ± 1.3
7b	62.6 ± 2.5	23.8 ± 1.3	37.2 ± 2.7	39.2 ± 2.4
7c	8.0 ± 1.6	1.5 ± 0.9	3.6 ± 1.3	16.9 ± 1.4
7e	7.5 ± 1.1	10.2 ± 2.7	9.1 ± 1.4	13.6 ± 2.4
7f	18.9 ± 2.1	11.7 ± 1.3	12.7 ± 1.9	6.8 ± 1.7
7g	2.9 ± 1.1	11.0 ± 1.9	10.1 ± 2.7	11.8 ± 1.6
7h	61.0 ± 1.9	26.3 ± 1.4	33.2 ± 1.7	38.5 ± 2.8
7i	16.7 ± 1.1	3.7 ± 1.8	11.6 ± 1.2	22.6 ± 1.5
carboxin	38.0 ± 2.0	120.3 ± 2.3	–	117.1 ± 3.2
penthiopyrad	71.9 ± 1.7	69.6 ± 2.4	74.4 ± 3.1	>200

[a]Values are mean ± SD of three replicates. "–" not tested.

Table 3. IC_{50} values of 4c, 5f and 7f against *P. infestans* SDH[a]

compound number	IC_{50} (μg/mL)
4c	12.5 ± 1.9 c
5f	135.3 ± 3.5 b
7f	3.8 ± 1.7 c
penthiopyrad	223.9 ± 20.9 a

[a]Different lower case letters (a, b, and c) in a column indicate significant differences between mean values evaluated by Duncan's multiple range test ($P < 0.05$).

character. The N(2)—N(1)—C(6), C(15)—N(4)—C(14) and C(8)—C(11)—N(3) bond angles were 117.45°, 116.46°, and 113.97°, respectively. The supplementary data for **4c** have been deposited in the Cambridge Crystallographic Data Centre (http://www.ccdc.cam.ac.uk/conts/retrieving.html) under deposition number 880862. The crystallographic data of title compound **4c** are provided in Table S1 in the Supporting Information.

Antifungal Activity. The preliminary antifungal activity results of the title compounds against six plant phytogenic fungi (*G. zeae*, *C. mandshurica*, *F. oxysporum*, *B. cinerea*, *P. infestans*, and *S. sclerotiorum*) at 100 μg/mL are shown in Table 1. As indicated in Table 1, some title compounds exhibited excellent antifungal activity against *G. zeae*, *C. mandshurica*, *F. oxysporum*, and *P. infestans* at 100 μg/mL. Among theses compounds, **4g** and **7a** exhibited 100% inhibition against *F.*

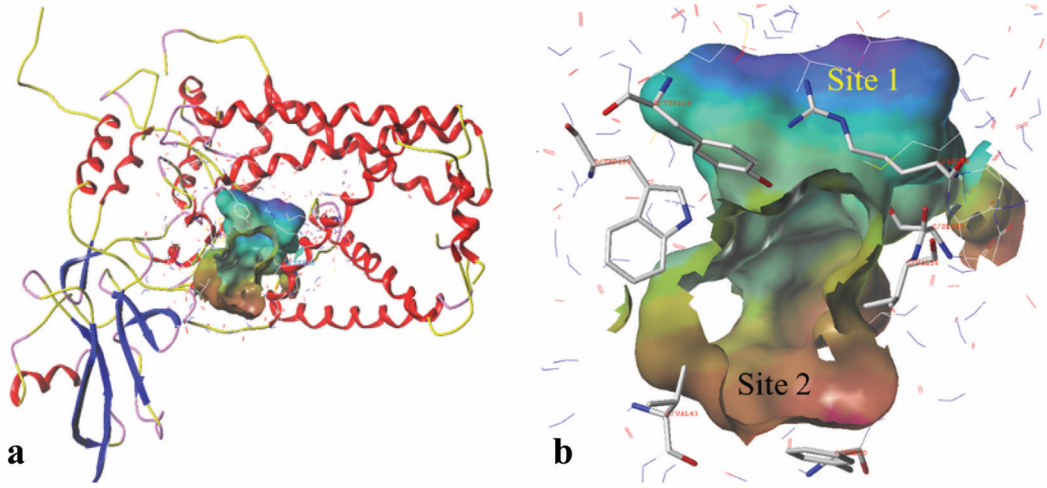

Figure 5. (a) *Pi*SDH structure obtained from homology modeling, and (b) the binding pocket depicted by the electrostatic potential map. The electronegative region is represented in blue, while the electropositive region is represented in red.

https://dx.doi.org/10.1021/acs.jafc.0c05702
J. Agric. Food Chem. 2021, 69, 1214−1223

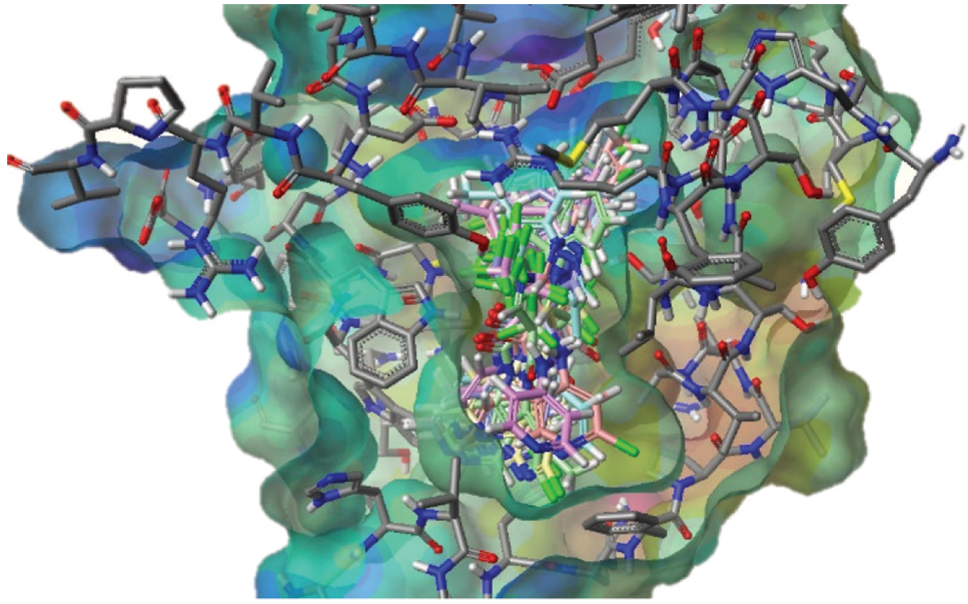

Figure 6. Docking poses of 20 ligands in the binding pockets of *P. infestans*.

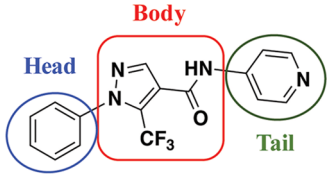

Figure 7. Ligand was divided into three fragments, namely, head (phenyl), body (5-trifluoromethyl pyrazole-4-carboxamide), and tail (pyridine).

oxysporum, **4g**, **7a**, and **7g** exhibited 100% inhibition against *C. mandshurica*, and **4c**, **4g**, and **7a** exhibited 100% inhibition against *P. infestans*. As shown in Table 2, the EC_{50} values of **4g**, **7a**, **7c**, **7e**, and **7g** against *G. zeae* were 9.6, 1.8, 8.0, 7.5, and 2.9 μg/mL, respectively, which were obviously superior to those of carboxin (38.0 μg/mL) and penthiopyrad (71.9 μg/mL). The EC_{50} values of **4g**, **7a**, **7c**, and **7i** against *F. oxysporum* were 8.4, 9.5, 1.5, and 3.7 μg/mL, respectively, which were much better than those of carboxin (120.3 μg/mL) and penthiopyrad (69.6 μg/mL). The EC_{50} values of **7a**, **7c**, and **7e** against *C. mandshurica* were 8.7, 3.6, and 9.1 μg/mL, respectively, which were superior to that of penthiopyrad (74.4 μg/mL). The EC_{50} values of **4c**, **4g**, **7a**, **7c**, and **7f** against *P. infestans* were 7.9, 7.2, 8.9, and 6.8 μg/mL, respectively, which were much better than that of carboxin (117.1 μg/mL). Preliminary structure−activity relationship (SAR) analysis revealed that the title compounds exhibited good antifungal activity when 4-pyridinyl was introduced to the amine moiety of the pyrazole carboxamide structure, and a phenyl group was introduced at the 1-position

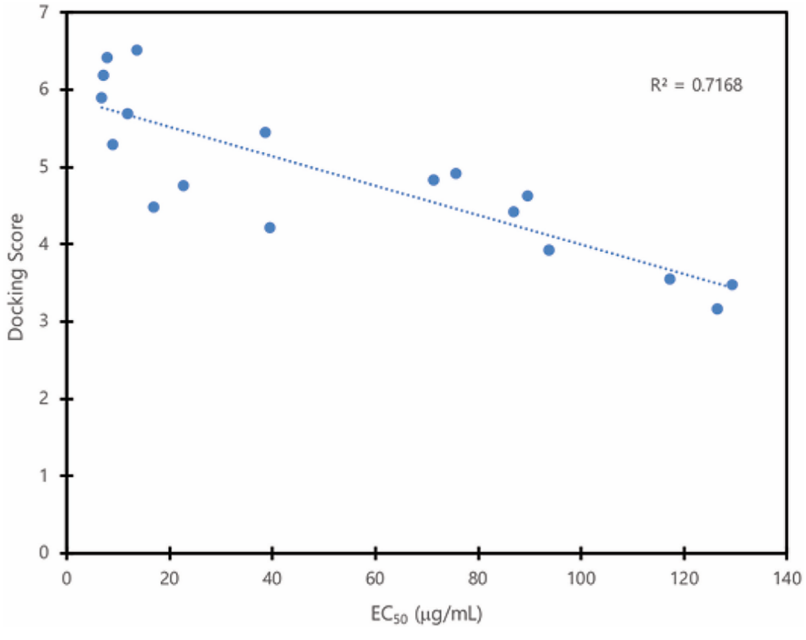

Figure 8. Linear relationship between the docking score and EC_{50} value that was studied for this series of title compounds.

https://dx.doi.org/10.1021/acs.jafc.0c05702
J. Agric. Food Chem. 2021, 69, 1214−1223

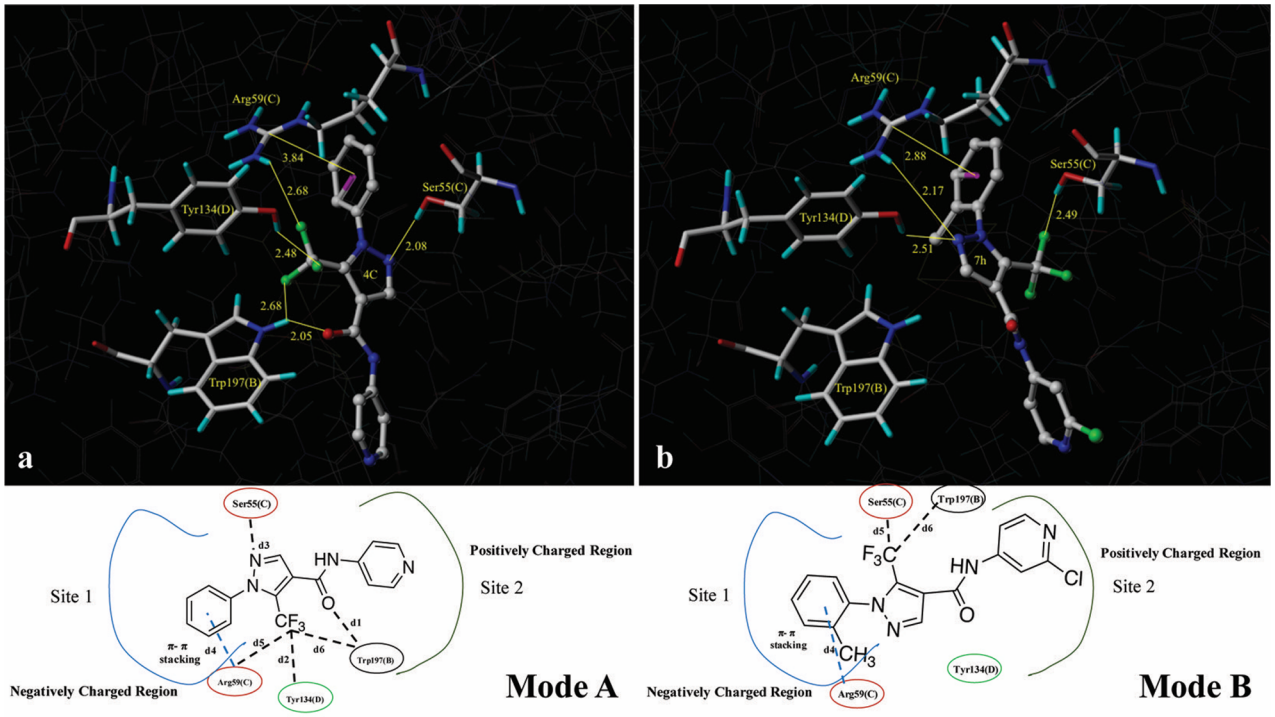

Figure 9. Docking poses of ligands (a) **4c** (mode A) and (b) **7h** (mode B) in the binding pocket of *P. infestans*.

of the pyrazole ring, such as in **4c**. However, compounds **7a**, **7e**, and **7g** exhibited excellent antifungal activity against four plant phytogenic fungi, because CH_3, Cl, or F was introduced to the adjacent position of the phenyl group in these compounds. Considering that CH_3 was introduced to the adjacent position of the pyridinyl of the amine, compounds **4g**, **7c**, **7f**, and **7g** exhibited excellent antifungal activity against the four plant phytogenic fungi.

Enzymatic Inhibition Activity of SDH. Compounds **4c**, **5f**, and **7f** were selected and evaluated for SDH enzymatic inhibition determination for target site validation. As shown in Table 3, **4c** and **7f** exhibited good SDH inhibition with IC_{50} values of 12.5 and 6.9 μg/mL, respectively, but **5f** exhibited low SDH inhibition with an IC_{50} value of 135.3 μg/mL. The IC_{50} value of penthiopyrad was 223.9 μg/mL.

SDH Model Analysis. The three-dimensional structure of the *Pi*SDH protein (PDB: 1ZOY, ID% = 49.9) obtained from the homology modeling studies is depicted in Figure 5a. The binding site depicted in Figure 5b shows that the pocket size was 866.4 Å^3. Moreover, the binding pocket consisted of more than nine residues from subunits B and C and only a few residues from subunit D, and the pocket was located in a similar position compared with the available sequence data (see the details in Table S4 in the Supporting Information).

Molecular Modeling Study. To elucidate the mechanism of potential SDH inhibitors and explain the SAR in detail, we performed docking studies. As shown in Figure 5b, the electrostatic potential maps can be easily classified in the *Pi*SDH model; the top part of the binding pocket (site 1) belongs to the electronegative region, whereas the bottom part (site 2) belongs to the electropositive region. The docking results for 20 ligands are depicted in Figure 6. The head fragment is oriented toward the negatively charged region (site 1), whereas the tail fragment is oriented toward the positively charged region (site 2) to match the characteristics of the binding pocket (Figure 7). A plot of the docking score versus EC_{50} value is shown in Figure 8, and it shows a linear relationship between the computed and experimental results with a regression coefficient (R^2) of 0.72. The detailed analysis of Figure 6 demonstrated two distinct docking poses (Figures S11− S15) for all docking structures (docking scores are summarized in Table S5 in the Supporting Information). The docking modes for **4c** (mode A) and **7h** (mode B) are shown in Figure 9. Among the 20 ligands, 15 ligands (**4c**, **4d**, **4e**, **4f**, **4g**, **5b**, **5f**, **5g**, **6f**, **7a**, **7b**, **7c**, **7e**, **7f**, and **7g**) were mode A binders while the five other ligands (**6b**, **6d**, **6g**, **7h**, and **7i**) were mode B binders, in which the pyrazole ring was rotated by 180°.

In mode A, the polar groups (CF_3, C═O, and N^2—pyrazole) in the body fragment formed H bonds and the phenyl ring showed $\pi-\pi$ interactions with Arg59. Ligand **4c** formed five H bonds (2.05−2.68 Å) with Ser55, Arg59, Tyr134, and Trp197 and a $\pi-\pi$ interaction between the phenyl ring and Arg59; the distance between the center of the phenyl ring and the central carbon connecting the three nitrogen atoms of Arg59 was 3.84 Å (Figure 9a). By introducing substituents into the head and tail fragments, the steric repulsion and electronegativity could induce a subtle change in the docking pose and the score. For instance, when a substituent was introduced into the 3-pyridyl position (**4d**, **4e**, and **4f**), the ligand moved upward to alleviate steric repulsion with the site 2 pocket, thus decreasing the docking score and increasing the EC_{50} value. In other words, the antifungal activity of the compounds was significantly reduced. The docking scores of these ligands were partly compensated by the electronegativity and increased according to the order Cl > Br > C. Considering that the 2-CH_3 substituent in the pyridine ring (**4g**) experienced less repulsion with the binding pocket, its docking score was slightly smaller than that of **4c**, thus improving the antifungal activity of **4g**. When two substituents were introduced into the phenyl and pyridine rings, two interactions could operate together. (1) The 3-

https://dx.doi.org/10.1021/acs.jafc.0c05702
J. Agric. Food Chem. 2021, 69, 1214−1223

phenyl substituents in **6b**, **6d**, **6f**, and **6g** experienced the second strongest repulsion with the site 1 pocket. (2) The 2- and 3-pyridinyl substituents in **6b**, **6d**, and **6g** also have repulsive interactions with the site 2 pocket. Considering the insufficient space to accommodate these ligands in the binding pocket, the body fragment had to rotate to form another favorable pose in mode B. As shown in Figure 9b, the CF_3 group of **7h** formed H bonds with Ser55 (2.49 Å) and N^2—pyrazole formed H bonds with Arg59 (2.88 Å) and Tyr134 (2.51 Å). This configuration reduced the antifungal activity of these title compounds.

A detailed analysis of the docking results for this series of title compounds revealed that, when a substituent (CH_3, F or Cl) was introduced into the 2-phenyl position, compounds such as **7a**, **7e**, and **7g** exhibited enhanced antifungal activity against *P. infestans*. Moreover, when CH_3 was introduced into the 2-pyridinyl position, compounds **4g**, **7c**, **7f**, and **7i** exhibited better antifungal activity against *P. infestans*. These results are consistent with the result of the preliminary SAR analysis. Therefore, this molecular docking study could provide a benchmark for understanding the antifungal activity against the phytopathogenic fungus *P. infestans* and prompt us to develop more potent SDH inhibitors.

A series of novel *N*-(susbstituted pyridine-4-yl)-1-(substituted phenyl)-5-trifluoromethyl-1*H*-pyrazole-4-carboxamide derivatives **4a**−**4i**, **5a**−**5h**, **6a**−**6h**, and **7a**−**7j** was designed and synthesized to discover the potential SDH inhibitors. The bioassay results showed that some title compounds exhibited excellent antifungal activity against four phytopathogenic fungi (*G. zeae*, *F. oxysporum*, *C. mandshurica*, and *P. infestans*). The EC_{50} values were 1.8 μg/mL for **7a** against *G. zeae*, 1.5 and 3.6 μg/mL for **7c** against *F. oxysporium* and *C. mandshurica*, respectively, and 6.8 μg/mL for **7f** against *P. infestans*. SDH enzymatic activity testing revealed that the IC_{50} values of **4c**, **5f**, **7f**, and penthiopyrad were 12.5, 135.3, 6.9, and 223.9 μg/mL, respectively. The molecular docking of this series of title compounds with the SDH model demonstrated that the body fragment formed H bonds, and the phenyl ring showed $\pi-\pi$ interactions with Arg59, suggesting that these novel 5-trifluoromethyl-pyrazole-4-carboxamide derivatives might target SDH. A detailed analysis of the docking results revealed that, when a substituent (CH_3, F, or Cl) and CH_3 were introduced into the 2-phenyl and 2-pyridinyl positions, respectively, the antifungal activity of the title compounds was notably improved. However, when a substituent was introduced into the 3-phenyl and 3-pyridinyl positions, the title compounds exhibited reduced antifungal activity. These results could provide a benchmark for understanding the antifungal activity against the phytopathogenic fungus *P. infestans* and prompt us to develop more potent SDH inhibitors.

■ ASSOCIATED CONTENT

Supporting Information

The Supporting Information is available free of charge at https://pubs.acs.org/doi/10.1021/acs.jafc.0c05702.

Discussions of ^{1}H NMR, ^{13}C NMR, ^{19}F NMR, HRMS, and MS data and molecular docking analysis, tables of crystallographic data, regression equations, characteristics of SDH binding pockets of *P. infestans*, and docking scores, and figures of ^{1}H NMR, ^{13}C NMR, ^{19}F NMR, and HRMS spectra and docking modes (PDF)

■ AUTHOR INFORMATION

Corresponding Authors

Chan Kyung Kim − *Department of Chemistry and Chemical Engineering, Center for Design and Applications of Molecular Catalysts, Inha University, Incheon 22212, Korea;* orcid.org/0000-0002-4716-5553; Phone: +82-32-860-7684; Email: kckyung@inha.ac.kr; Fax: +82-32-867-5604

Song Yang − *State Key Laboratory Breeding Base of Green Pesticide and Agricultural Bioengineering, Key Laboratory of Green Pesticide and Agricultural Bioengineering, Ministry of Education, Center for R&D of Fine Chemicals of Guizhou University, Guiyang 550025, China;* orcid.org/0000-0003-1301-3030; Phone: +86-851-88292171; Email: jhzx.msm@gmail.com; Fax: +86-851-88292170

Authors

Zhibing Wu − *State Key Laboratory Breeding Base of Green Pesticide and Agricultural Bioengineering, Key Laboratory of Green Pesticide and Agricultural Bioengineering, Ministry of Education, Center for R&D of Fine Chemicals of Guizhou University, Guiyang 550025, China;* orcid.org/0000-0002-2724-9725

Hyung-Yeon Park − *Department of Chemistry and Chemical Engineering, Center for Design and Applications of Molecular Catalysts, Inha University, Incheon 22212, Korea*

Dewen Xie − *College of Pharmacy, Guizhou University, Guiyang 550025, China*

Jingxin Yang − *State Key Laboratory Breeding Base of Green Pesticide and Agricultural Bioengineering, Key Laboratory of Green Pesticide and Agricultural Bioengineering, Ministry of Education, Center for R&D of Fine Chemicals of Guizhou University, Guiyang 550025, China*

Shuaitao Hou − *State Key Laboratory Breeding Base of Green Pesticide and Agricultural Bioengineering, Key Laboratory of Green Pesticide and Agricultural Bioengineering, Ministry of Education, Center for R&D of Fine Chemicals of Guizhou University, Guiyang 550025, China*

Nasir Shahzad − *Department of Chemistry and Chemical Engineering, Center for Design and Applications of Molecular Catalysts, Inha University, Incheon 22212, Korea*

Complete contact information is available at: https://pubs.acs.org/10.1021/acs.jafc.0c05702

Author Contributions

‖Z.W. and H.-Y.P. should be considered joint first authors.

Funding

This work was supported by the National Natural Science Foundation of China (Nos. 21662008 and 21877021), the Key Technologies R&D Program (No. 2014BAD23B01), and the Science and Technology Project of Guizhou province (No. [2017]5788).

Notes

The authors declare no competing financial interest.

■ ACKNOWLEDGMENTS

C.K.K. would like to thank Inha University for support of this work.

■ REFERENCES

(1) Xiong, L.; Shen, Y. Q.; Jiang, L. N.; Zhu, X. L.; Yang, W. C.; Huang, W.; Yang, G. F. Succinate Dehydrogenase: An Ideal Target for Fungicide Discovery. In *Discovery and Synthesis of Crop Protection*

Products; Maienfisch, P., Stevenson, T. M., Eds.; American Chemical Society: Washington DC, 2015; pp 175−194.
(2) Schmeling, B. V.; Kulka, M. Systemic Fungicidal Activity of 1,4-Oxathiin Derivatives. *Science* **1966**, *152*, 659−660.
(3) Horsefield, R.; Yankovskaya, V.; Sexton, G.; Whittingham, W.; Shiomi, K.; Omura, S.; Byrne, B.; Cecchini, G.; Iwata, S. Structural and computational analysis of the quinone-binding site of complex II (succinate-ubiquinone oxidoreductase): a mechanism of electron transfer and proton conduction during ubiquinone reduction. *J. Biol. Chem.* **2006**, *281*, 7309−7316.
(4) Culbreath, A. K.; Brenneman, T. B.; Kemerait, R. C., Jr; Hammes, G. G. Effect of the new pyrazole carboxamide fungicide penthiopyrad on late leaf spot and stem rot of peanut. *Pest Manage. Sci.* **2009**, *65*, 66−73.
(5) Avenot, H. F.; Michailides, T. J. Progress in understanding molecular mechanisms and evolution of resistance to succinate dehydrogenase inhibiting (SDHI) fungicides in phytopathogenic fungi. *Crop Prot.* **2010**, *29*, 643−651.
(6) Mathre, D. E. Mode of Action of Oxathiin Systemic Fungicides: III. Effect on Mitochondrial Activities. *Pestic. Biochem. Physiol.* **1971**, *1*, 216−224.
(7) Araki, F.; Yabutani, K. Development of a systemic fungicide, Flutolanil. *J. Pestic. Sci.* **1993**, *18*, 69−77.
(8) Bergdahl, D. R.; French, D. W. Systemic fungicide benodanil for control of pine-oak rust on pine seedlings in the nursery. *Plant Dis.* **1984**, *68*, 225−256.
(9) Glättli, A.; Grote, T.; Stammler, G. SDH-Inhibitors: History, Biological Performance and Molecular Mode of Action. *Modern fungicides and antifungal compounds VI*, Proceedings of the 16th International Reinhardsbrunn Symposium, Friedrichroda, Germany, April 25−29, 2011; pp 159−169.
(10) Sierotzki, H.; Scalliet, G. A Review of Current Knowledge of Resistance Aspects for the Next-Generation Succinate Dehydrogenase Inhibitor Fungicides. *Phytopathology* **2013**, *103*, 880−887.
(11) Wei, G.; Gao, M. Q.; Zhu, X. L.; Yang, G. F. Research progress on carboxamide fungicides targeting succinate dehydrogenase. *Chin. J. Pestic. Sci.* **2019**, *21*, 673−680.
(12) Zeun, R.; Scalliet, G.; Oostendorp, M. Biological activity of sedaxane: a novel broad-spectrum fungicide for seed treatment. *Pest Manage. Sci.* **2013**, *69*, 527−534.
(13) Piqueras, C. M.; Latorre, B. A.; Torres, R. Effectiveness of isofetamid, a new succinate dehydrogenase inhibitor fungicide, in the control of grapecine gray mold. *Cienc. Inv. Agr.* **2014**, *41*, 17−18.
(14) Hou, Y. P.; Mao, X. W.; Wang, J. X.; Zhan, S. W.; Zhou, M. G. Sensitivity of Fusarium asiaticum to a novel succinate dehydrogenase inhibitor fungicide pydiflumetofen. *Crop Prot.* **2017**, *96*, 237−244.
(15) Ackrell, B. A. C. Progress in understanding structure-function relationships in respiratory chain complex II. *FEBS Lett.* **2000**, *466*, 1−5.
(16) Omura, S.; Shiomi, K. Discovery, chemistry, and chemical biology of microbial products. *Pure Appl. Chem.* **2007**, *79*, 581−591.
(17) Ito, Y.; Muraguchi, H.; Seshime, Y.; Oita, S.; Yanagi, S. O. Flutolanil and carboxin resistance in Coprinus cinereus conferred by a mutation in the cytochrome b_{560} subunit of succinate dehydrogenase complex (Complex II). *Mol. Genet. Genomics* **2004**, *272*, 328−335.
(18) Cecchini, G. Function and Structure of Complex II of the Respiratory Chain. *Annu. Rev. Biochem.* **2003**, *72*, 77−109.
(19) Huang, L. S.; Sun, G.; Cobessi, D.; Wang, A. C.; Shen, J. T.; Tung, E. Y.; Anderson, V. E.; Berry, E. A. 3-Nitropropionic Acid Is a Suicide Inhibitor of Mitochondrial Respiration That, upon Oxidation by Complex II, Forms a Covalent Adduct with a Catalytic Base Arginine in the Active Site of the Enzyme. *J. Biol. Chem.* **2006**, *281*, 5965−5972.
(20) Inaoka, D. K.; Shiba, T.; Sato, D.; Balogun, E. O.; Sasaki, T.; Nagahama, M.; Oda, M.; Matsuoka, S.; Ohmori, J.; Honma, T.; Inoue, M.; Kita, K.; Harada, S. Structural insights into the molecular design of flutolanil derivatives targeted for fumarate respiration of parasite mitochondria. *Int. J. Mol. Sci.* **2015**, *16*, 15287−15308.
(21) Ruprecht, J.; Iwata, S.; Rothery, R. A.; Weiner, J. H.; Maklashina, E.; Cecchini, G. Perturbation of the Quinone-binding Site of Complex II Alters the Electronic Properties of the Proximal [3Fe-4S] Iron-Sulfur Cluster. *J. Biol. Chem.* **2011**, *286*, 12756−12765.
(22) Ruprecht, J.; Yankovskaya, V.; Maklashina, E.; Iwata, S.; Cecchini, G. Structure of Escherichia coli Succinate:Quinone Oxidoreductase with an Occupied and Empty Quinone-binding Site. *J. Biol. Chem.* **2009**, *284*, 29836−29846.
(23) Wu, Z. B.; Hu, D. Y.; Kuang, J. Q.; Cai, H.; Wu, S. X.; Xue, W. Synthesis and antifungal activity of *N*-(substituted pyridinyl)-1-methyl(phenyl)-3-(trifluoromethyl)-1H-pyrazole-4-carboxamide derivatives. *Molecules* **2012**, *17*, 14205−14218.
(24) Yang, W. Q.; Zhou, X.; Wu, Z. B. Design, Synthesis, Antifungal and Antibacterial Activities of *N*-phenyl and N-pyridinyl-5-(trifluoromethyl)-pyrazole-4-carboxamide Derivatives. *J. Heterocyclic Chem.* **2018**, *55*, 2261−2269.
(25) Wang, X. J.; Magnuson, S.; Pastor, R.; Fan, E.; Hu, H. Y.; Tsui, V.; Deng, W.; Murray, J.; Steffek, M.; Wallweber, H.; Moffat, J.; Drummond, J.; Chan, G.; Harstad, E.; Ebens, A. J. Discovery of novel pyrazolo 1,5-a pyrimidines as potent pan-Pim inhibitors by structure- and property-based drug design. *Bioorg. Med. Chem. Lett.* **2013**, *23*, 3149−3153.
(26) Rosen, M. D.; Venkatesan, H.; Peltier, H. M.; Bembenek, S. D.; Kanelakis, K. C.; Zhao, L. X.; Leonard, B. E.; Hocutt, F. M.; Wu, X. D.; Palomino, H. L.; Brondstetter, T. I.; Haugh, P. V.; Cagnon, L.; Yan, W.; Liotta, L. A.; Young, A.; Mirzadegan, T.; Shankley, N. P.; Barrett, T. D.; Rabinowitz, M. H. Benzimidazole-2-pyrazole HIF Prolyl 4-Hydroxylase Inhibitors as Oral Erythropoietin Secretagogues. *ACS Med. Chem. Lett.* **2010**, *1*, 526−529.
(27) Xu, W. M.; He, J.; He, M.; Han, F. F.; Chen, X. H.; Pan, Z. X.; Wang, J.; Tong, M. G. Synthesis and Antifungal Activity of Novel Sulfone Derivatives Containing 1,3,4-Oxadiazole Moieties. *Molecules* **2011**, *16*, 9129−9141.
(28) Li, P.; Shi, L.; Yang, X.; Yang, L.; Chen, X. W.; Wu, F.; Shi, Q. C.; Xu, W. M.; He, M.; Hu, D. Y.; Song, B. A. Design, synthesis, and antibacterial activity against rice bacterial leaf blight and leaf streak of 2,5-substituted-1,3,4-oxadiazole/thiadiazole sulfone derivative. *Bioorg. Med. Chem. Lett.* **2014**, *24*, 1677−1680.
(29) Guo, X. F.; Zhao, B.; Fan, Z. J.; Yang, D. Y.; Zhang, N. L.; Wu, Q. F.; Yu, B.; Zhou, S.; Kalinina, T. A.; Belskaya, N. P. Discovery of Novel Thiazole Carboxamides as Antifungal Succinate Dehydrogenase Inhibitors. *J. Agric. Food Chem.* **2019**, *67*, 1647−1655.
(30) Shi, J.; Blundell, T. L.; Mizuguchi, K. FUGUE: sequence-structure homology recognition using environment-specific substitution tables and structure-dependent gap penalties. *J. Mol. Biol.* **2001**, *310*, 243−257.
(31) Mizuguchi, K.; Deane, C. M.; Blundell, T. L.; Overington, J. P. HOMSTRAD: a database of protein structure alignments for homologous families. *Protein Sci.* **1998**, *7*, 2469−2471.
(32) Montalvao, R. W.; Smith, R. E.; Lovell, S. C.; Blundell, T. L. CHORAL: a differential geometry approach to the prediction of the cores of protein structures. *Bioinformatics* **2005**, *21*, 3719−3725.
(33) Schrauber, H.; Eisenhaber, F.; Argos, P. Rotamers: To be or not to be? An analysis of amino acid side-chain conformations in globular proteins. *J. Mol. Biol.* **1993**, *230*, 592−612.
(34) Mannhold, R.; Rekker, R. F.; Sonntag, C.; Ter Laak, A. M.; Dross, K.; Polymeropoulos, E. E. Comparative Evaluation of the Predictive Power of Calculation Procedures for Molecular Lipophilicity. *J. Pharm. Sci.* **1995**, *84*, 1410−1419.
(35) Kim, C.; Kim, J.; Park, H. Y.; Park, H. J.; Lee, J. H.; Kim, C. K.; Yoon, J. Furanone derivatives as quorum-sensing antagonists of Pseudomonas aeruginosa. *Appl. Microbiol. Biotechnol.* **2008**, *80*, 37−47.
(36) Kim, C.; Kim, J.; Park, H. Y.; Lee, J. H.; Park, H. J.; Kim, C. K.; Yoon, J. Structural understanding of quorum-sensing inhibitors by molecular modeling study in Pseudomonas aeruginosa. *Appl. Microbiol. Biotechnol.* **2009**, *83*, 1095−1103.
(37) Kim, C.; Kim, J.; Park, H. Y.; Park, H. J.; Kim, C. K.; Yoon, J.; Lee, J. H. Development of inhibitors against TraR quorum-sensing

https://dx.doi.org/10.1021/acs.jafc.0c05702
J. Agric. Food Chem. 2021, 69, 1214−1223

system in Agrobacterium tumefaciens by molecular modeling of the ligand-receptor interaction. *Mol. Cells* **2009**, *28*, 447−453.

https://dx.doi.org/10.1021/acs.jafc.0c05702
J. Agric. Food Chem. 2021, 69, 1214−1223